



---

## ***Chapter VII***

### **Physicochemical and Microstructural Changes in Nonaoxyethylene n-Dodecyl Ether in Aqueous-Amino Acids Region: Tensiometric, Small Angle Neutron Scattering, Dynamic Light Scattering and Rheological Studies**

---

Solubility, tensiometric, small-angle neutron scattering (SANS), dynamic light scattering (DLS) and viscometric measurements have been used to elucidate the solution and morphological properties of Nonaoxyethylene *n*-dodecyl ether [CH<sub>3</sub>(CH<sub>2</sub>)<sub>11</sub> (OCH<sub>2</sub>CH<sub>2</sub>)<sub>9</sub>OH], C<sub>12</sub>E<sub>9</sub> over a limited range of temperature, surfactant concentration, both in presence and absence of amino acids. Phase diagram for the aqueous solution of C<sub>12</sub>E<sub>9</sub> (0.1% to 40% (w/v)) and in the presence of amino acids were constructed by clouding temperature measurements. Critical micelle concentrations (CMC) were determined by the surface tension measurement in presence of glycine, alanine, and valine. It can be concluded that the structure breaking ability of amino acids and its interaction with the oxyethylene group of the surfactant are dominating factor in the micellization process. SANS measurements have been made to elucidate the microstructural information viz. aggregation number ( $N_{agg}$ ), shape, size and number density ( $n_m$ ) of C<sub>12</sub>E<sub>9</sub> micelle in D<sub>2</sub>O at different concentrations of amino acids (0.4, and 0.6M) and temperatures (30, 45 and 60°C). Intrinsic viscosity gives the hydrated micellar volume ( $V_h$ ), volume of the hydrocarbon core ( $V_c$ ) and the volume of the palisade layer of OE unit ( $V_{OE}$ ). SANS as well as rheological data support the formation of non-spherical micelle with or without amino acids at higher surfactant concentration. SANS data showed that the surfactant formed prolate ellipsoidal micelle with a constant size (in the concentration range of 5mM to 20mM) but the micelle registered a 60 - 70% increase in size, in the association number and the other micellar parameter (i.e. the number density of micelles changed inversely with the rise in temperature) from 30 to 60°C rise in temperature. The hydrodynamic radius,  $R_h$  and the size distribution in terms of translational diffusion coefficient,  $D_o$  of the micelles were obtained from the analysis of the time correlation function of the scattering intensity measured at multiangle scattering of 50° to 130° and for different concentrations and temperatures (30, 45 and 55°C) as did in SANS. The values of hydrodynamic radius of micelle ( $R_h$ )

decrease on increasing the concentration of surfactant and on increasing the temperatures.

## INTRODUCTION

The self-association of surfactant molecules into finite sized molecular aggregates such as micelles in aqueous solution is significant for their numerous uses. The nonionic polyoxyethylene ether,  $C_nE_m$  are often taken in both fundamental and applied research interest due to its ever-growing applicability in numerous fields of industrial and commercial applications like detergency, food and dye stuff, deinking, agro and petrochemical, cosmetic etc as well as in electronic, cancer research and in drug delivery and will continue in the future due to their reasonably high solubility at low temperature. The physicochemical and microstructural properties of surfactant are very sensitive and are influenced or tuned to desire range, shape and application by altering the structure of surfactant monomer,<sup>1</sup> and the solution condition such as concentration, solvent polarity and type, temperature, pressure,  $pH$  and the presence of various foreign substances (co-solute).<sup>2-12</sup> The presence of an additional component in the surfactant solution alters the micellization process to a greater extent especially in the two ways<sup>13,14</sup> i) through specific interaction with the surfactant molecules, ii) by changing the solvent nature.

Such aggregates are formed in various shapes e.g. globular, ellipsoidal, cylindrical and disc like.<sup>15</sup> Control of the morphology of such aggregates by the addition of external additives or by proper choice of surfactant mixture has become increasingly important in recent years from both the theoretical and experimental points of view.

To achieve a deep understanding of physico-chemical properties of micelle, both the dynamic and morphological properties must be achieved simultaneously.<sup>16</sup> There is no single technique capable of yielding both types of information unambiguously, thus, there is a need to combine both the studies in

order to gather the information. The nature of co-solute decides the direction of the changes in the CMC of the surfactants. The co-solutes may be distributed between aqueous and micellar phase and may accumulate both in the palisade layer and inside the micelle hydrophobic core, thus favoring the stability of the system. Electrolytes generally decrease the CMC,<sup>17</sup> nonelectrolytes may increase or decrease,<sup>18</sup> some organic co-solutes which when present in some greater amounts may even cause disappearance of the micelles.<sup>19</sup>

Amino acids are zwitterionic biomolecules and are the basic unit of protein.<sup>20</sup> They have common hydrophilic groups and various kinds of side chains of different hydrophobicities. Also they are considered to be strong structure breakers in aqueous solution due to the presence of peripheral charges.<sup>20</sup> They are also expected to undergo strong electrostatic interactions with charged species in aqueous solution. Hatton et al.<sup>21-23</sup> have discussed on the phenomenon of solubilization in reversed micelle using various amino acids as model molecules. They showed from phase transfer experiment that the hydrophilic amino acids such as glycine and threonine are solubilized only in the water pool, where as hydrophobic amino acid such as tyrosine are taken up both in the water pool and in the interfacial zone. However Adachi et al.<sup>24</sup> also did the same study in sodium bis (2-ethyl hexyl) sulposuccinate (AOT) in reverse micelle, but they conclude that the hydrophilic amino acids are taken up only in the water pool through electrostatic interaction, and the amino acids with strongly hydrophobic groups are mainly incorporated in the interfacial layer of the globule through the hydrophobic interaction. Bakshi et al.<sup>25</sup> also investigated the limited solution properties of different amino acid on sodium dodecylsulphate (SDS) and dodecyl trimethylammmonium bromide (DTAB) surfactants. Tantone et al.<sup>26</sup> carried out some physicochemical properties of Octyl  $\beta$ -D-glycopyranoside (OBG) micelles in presence of glycine. They found significant increase of the minimum area per polar head group of OBG molecules and a shift of the cmcs towards lower values were observed. In addition they observed smooth increase of the hydrodynamic

size of the micellar aggregates by viscometric measurements. To explain such features two different working hypothesis have been made, (1) a direct interaction between nonionic micelle and amino acid at the micellar interface leading to the adsorption of amino acid on the micelles<sup>27</sup> and (2) a modification of the micellar aggregation properties due to thermodynamic conditions of the solvent mixture.<sup>28</sup> In order to discriminate between these two hypothesis we have undertaken the present study. Also seen that most of the publications referred above, address the possible effect of amino acids on ionic surfactants, however, we have not seen a comprehensive physicochemical and morphological study of nonionic, nonaoxyethylene mono *n*-dodecyl ether, C<sub>12</sub>E<sub>9</sub> surfactant in presence of amino acids. Hence we studied the phase separation, solution, small angle neutron scattering (SANS), viscosity and dynamic light scattering (DLS) properties of C<sub>12</sub>E<sub>9</sub>-aqueous-amino acids ternary system.

## EXPERIMENTAL SECTION

**Materials.** C<sub>12</sub>E<sub>9</sub>, [MW=582.85, Lion corporation, Tokyo, Japan], was used without further purification. glycine (gly), alanine (ala) and valine (val) (Merck, AR) were recrystallized from alcohol-water mixture<sup>29</sup> and dried *in vacuo* before use. For physicochemical properties, all solutions were prepared by using triple distilled deionized water, showing electric conductance 2-3  $\mu\text{S cm}^{-1}$  at 303K. For DLS experiments the milli Q water and for SANS study, solvent D<sub>2</sub>O (99.4%, Heavy water division, BARC, Mumbai) was used.

**Methods.** The Surface tension ( $\gamma$ ) was measured by du-Noüy ring tensiometer (S. C. Dey and Co. Kolkata, India) at 35°C and in amino acid solutions of various concentrations (%) viz. 0.1, 0.25, 0.5, 0.75 and 1.0. Temperatures were maintained ( $\pm 0.1\text{K}$ ) constant by circulating thermostated water through a jacketed vessel containing the solution. Other conditions were same as reported in our recent papers.<sup>7,11,30,31</sup>

SANS is an ideal, noninvasive technique for determining the micellar morphology<sup>32</sup> and this has been also demonstrated for surfactant solution in presence of various additives.<sup>33</sup> SANS experiments were carried out on the micellar solutions prepared by dissolving known amount of surfactant in D<sub>2</sub>O. The use of D<sub>2</sub>O instead of water for preparing solution for SANS experiments was because this provides a very good contrast between the micelles and the solvent. SANS experiments were performed on the SANS instrument at the DHRUVA reactor, Trombay, Mumbai, India.<sup>34</sup> The instrument makes use of a BeO filter to obtain a monochromatic beam. The mean wavelength of the incident neutron beam  $\lambda$  is 5.2 Å with a wavelength resolution ( $\Delta\lambda/\lambda$ ) of approximately 15%. The scattered neutrons are detected in an angular range of 0.5-15° using one-dimensional linear position sensitive detector (PSD). The accessible wave vector transfer,  $Q$  ( $=4\pi\sin\theta/\lambda$ , where  $2\theta$  is the scattering angle and  $\lambda$  is the wavelength of the incident neutrons) in above instrument is 0.018 Å<sup>-1</sup> to 0.30 Å<sup>-1</sup>. PSD allows simultaneous recording of the data over the full  $Q$  range. The solutions were held in a 0.5 cm path length UV-grade quartz cell with tight fitting teflon stoppers. The SANS data were recorded at 30, 45 and 60°C ( $\pm 0.2^\circ$ ). At a given temperature, the concentrations of the surfactant and amino acid were varied. In all the data, scattering intensities were corrected for the background and the solvent scattering and normalized to absolute cross-section units. Thus a plot of cross section per unit volume ( $\partial\Sigma/\partial\Omega$ ) vs scattering vector ( $Q$ ) were obtained. DLS measurements were carried out for C<sub>12</sub>E<sub>9</sub> amino acids systems at five different scattering angles (50, 70, 90, 110 and 130°) using a Malvern 4800 photon correlation spectrometer. The instrument is equipped with a 2 W argon ion laser ( $\lambda = 514.5$  nm) with a vertically polarized light. All measurements were carried out at an output power of 250 mW and at 30, 45 and 55°C ( $\pm 0.1^\circ$ C). The surfactant solutions were filtered through 0.2 µ Acrodis Teflon filter directly in to the sample cell and sealed until used. The intensity correlation function was measured 5 times for each sample at

each angle. The average decay rate was obtained from the measured autocorrelation function using the method of cumulants employing a quadratic fit<sup>35</sup> and the error in these repeated measurements was approximately 5%.

The viscosity of surfactant solution arises because of the interaction of both the hydrophobic core and hydrophilic outer shell of the micelle with water. It measures the solute-solvent interaction as well as the shape and size of the micelle. The latter are effected by temperature changes. Thus, we determine the viscosity of C<sub>12</sub>E<sub>9</sub> surfactant solution in absence and presence of amino acids and the temperatures as we did for SANS and DLS measurements. The flow time of surfactant solution and water were measured with the help of an Ubbelohde suspended level viscometer.<sup>11</sup> Density of surfactant solution has been determined with a pycnometer. Density and viscosity measurements were carried out in a thermostated water bath ( $\pm 0.1^\circ\text{C}$ ). Samples were carefully filtered before injection into viscometer. Three consecutive flow times agreeing within  $\pm 0.2\text{s}$  were taken and the mean flow time was considered.

The phase separation of surfactant solution is studied by determination of Cloud Point (CP) temperatures of C<sub>12</sub>E<sub>9</sub> (0.1 –40% w/v) as well as 1% (w/v) aqueous surfactant solution in the presence of increasing amount of amino acids and was determined as described elsewhere.<sup>9</sup> The CP are average of the temperature at which clouding appears and then disappears. These temperatures did not differ by greater than  $\pm 0.2^\circ\text{C}$ .

## RESULTS AND DISCUSSION

**Dilute Solution Phase Diagrams.** The phase diagrams for the dilute aqueous solutions of  $C_{12}E_9$  surfactant solution (in concentration range of 0.1-40% (w/v)) were constructed (Figure 1). The phase diagrams of  $C_{12}E_9$  aqueous surfactant solution both in absence as well as in presence of the additives have been characterized by the following common features: a given clear solution at room temperature were warmed, becomes cloudy upon heating across the entire solution volume. Solutions in the concentration range (0.1-40%) studied remain isotropic and clear initially, on heating it become cloudy, temperature at which clouds were noted is considered as the cloud point (CP). It is interesting to note that the clouds once formed remain stable with out any phase separation up to temperature close to 96°C.

For 1% (~17mM)  $C_{12}E_9$  solution the phase separation temperature i.e. cloud point was found to be 84°C, which is in good agreement to the reported value.<sup>9</sup> The CP increases as concentration decreases from dilute solution to very dilute solution (less than 1%, inset in Fig 1). However CP decreases as the concentration becomes greater than 1% up to about 6% (w/v). Above 8% (w/v) the CP increase with increasing the concentration of surfactant. The decrease in CP with increase in  $C_{12}E_9$  concentration is due to increase in micellar density as we observed in small angle neutron scattering study (SANS) explained in next section. It can be stated that the OE part (70.8%) of the  $C_{12}E_9$  is mainly responsible for over all solubility in water. The phase separation results from heightened micelle-micelle interaction. Also after a threshold temperature the phase separation occurred due to the sharp increase in the aggregation of the micelles and decrease in the inter micellar repulsions via dehydration of the polyoxyethylene hydrophilic group followed by the self-association. However at higher concentration (> 8%) the CP increase. Koshy<sup>36</sup> et al also observed the similar results for Triton X-100 and Triton X- 114, where they studied the surfactant concentration effect from 1 to 10% (w/v) on cloud point. The authors found the minimum around 3% in the CP-



concentration curve in both the surfactants. Similar results were obtained by Heusch<sup>37</sup>.

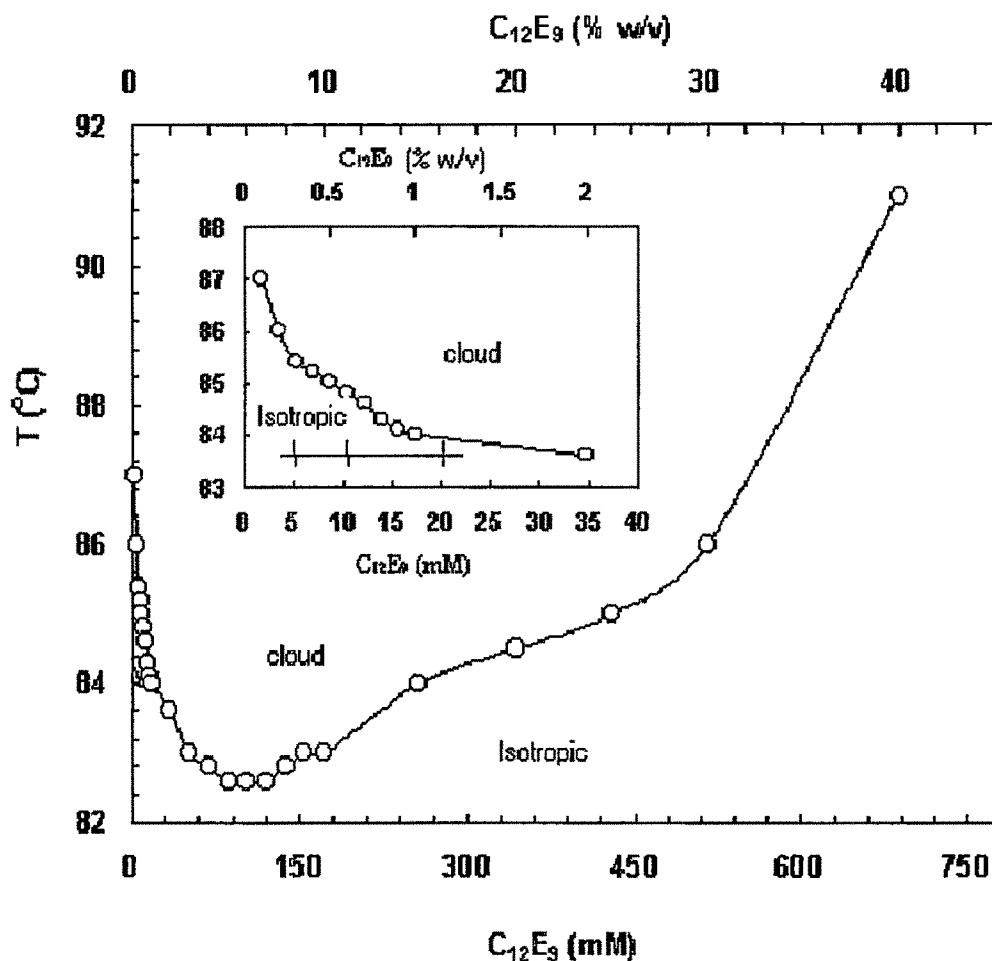


Figure 1. Dilute solution phase diagram of  $C_{12}E_9$  solution; (O) final cloud points

This is because, at high surfactant concentration, a structured water-surfactant system is present.<sup>37</sup> With increase in temperature, this structure breaks. Though the molecules are not free of the surfactant effect at this stage. In other words, some of the water molecules are attached to the micelle in particular but to the micelle system in general, forming a bridge between micelles. However the micelle are still separated because of the presence of these water molecules. It has been

suggested earlier that in polyglycol ether surfactant system the water molecules is available for total tenside molecules.<sup>38</sup> Therefore higher temperature is required to remove these “floating” water molecules which are barrier for micellar interaction. Once they move out at higher temperature the micelle-micelle interaction becomes easier. That is why the CP is seen at higher temperature and at this temperature the bridge water molecules are released.

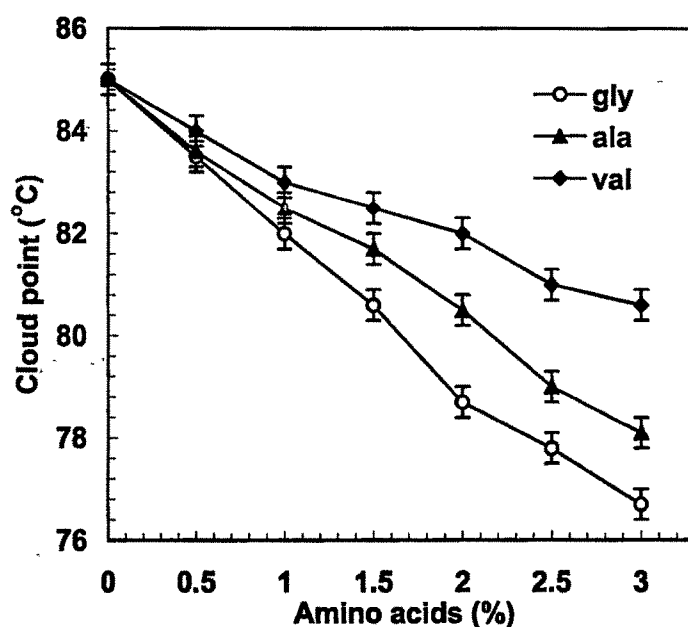


Figure 2. Cloud points of  $C_{12}E_9$  (1%w/v) in presence of amino acids.

Figure 2 show the phase separation of  $C_{12}E_9$  (1%, w/v) surfactant in the presence of increasing amounts of three amino acids gly, ala and val as cosolutes. It can be seen that phase separation occurs easily in the presence of amino acids, by decreasing the clouding temperature of  $C_{12}E_9$ . This is due to high solvation of amino acid zwitterions, they are solublized in outer regions of the micelle decrease the CP by decreasing the availability of non-associated water molecules to hydrate the ether oxygen of the POE chain. Hence micelles can become closed to each other easily. The ethylene oxide group of POE surfactant is highly hydrated. When the amino acids are added, the water of hydration of the micelle decreases, as these

additives compete for water molecules associated with the micelle. Thus with two relatively less hydrated micelles approaching each other, the hydration spheres overlap and some of the water molecules are freed to increase the entropy of the system. However, Rupert<sup>39</sup> suggested that the hydrophobic and hydrophilic parts of the micelle interact with water differently where temperature dependent interaction parameters come in to play. At CP the hydrophobicity has relative more dominance over hydrophilicity and complete removal of water may not be necessary. In the present study it is difficult to make a choice between two ideas. In any case the overall entropy is high and hence the free energy changes is relatively more negative and thus the phase separation is facile. It is known that the OE group is voluminous and relatively less hydrophilic. It needs about two  $-\text{OCH}_2\text{CH}_2-$  groups to balance three  $-\text{CH}_2-$  to make system sufficiently hydrophilic for water solubility.<sup>40</sup> Water molecule strongly interacts with amino acid as well as oxyethylene groups of  $\text{C}_{12}\text{E}_9$ . This competitive interaction between the surfactant solute and the additive cosolute for the water around them would also induce the breaking of the hydrogen bonds between the oxyethylene parts of the surfactant and water. These effects together are perhaps responsible for the observed lowering in the cloud points and also the boundary lines in the phase diagrams of the surfactant solutions. Among the amino acids used the order of the decreasing CP of  $\text{C}_{12}\text{E}_9$  is  $\text{gly} > \text{ala} > \text{val}$ . The explanation of the variation is given in next section.

In the present investigation, an attempt has been made through surface tension, SANS, DLS and viscosity measurements to characterize the micellar properties and structural information of  $\text{C}_{12}\text{E}_9$  surfactant in absence and in the presence of different amino acids in the region of the phase diagram corresponding to transparent and isotropic states. The range of concentrations (5, 10, 20mM) studied at a fixed temperature of 30°C and temperature variations (30, 45 and 55 or 60°C) at a fixed concentration (20mM) for SANS, DLS and viscosity measurements is shown as horizontal lines in inset in Figure 1.

### **Critical Micelle Concentration (CMC) and Surface-Active Properties.**

Micellization is the result of dual tendencies of surfactant molecules to collect at any interface where the hydrophobic group can be removed from the contact with water and the hydrophilic group can remain wetted. By this phenomenon the organic moiety comes together forming a liquid like core with the polar groups remaining exposed to the water. It is an entropy directed process. It is well known that London dispersion forces are the main attractive forces in the formation of the micelles and that the micelle formation is supposed to be the result of hydrophobic interaction.<sup>7</sup> The value of critical micellar concentration (CMC) of  $C_{12}E_9$  surfactant in presence and absence of amino acids are extracted from surface tension-log concentration plots along with various surface active properties such as surface pressure at cmc,  $\pi_{CMC}$ , surface excess concentration,  $\Gamma_{max}$ ,  $A_{min}$ , i.e the area at  $\pi_{CMC}$  the concentration at which the surface tension of water is reduced by 20 units,  $C_{20}$  and the ratio of  $CMC/C_{20}$  at 35°C are listed in Table 1. Representative plots of  $\gamma$  vs  $\log_{10} C$  isotherms are shown in Figure 3.

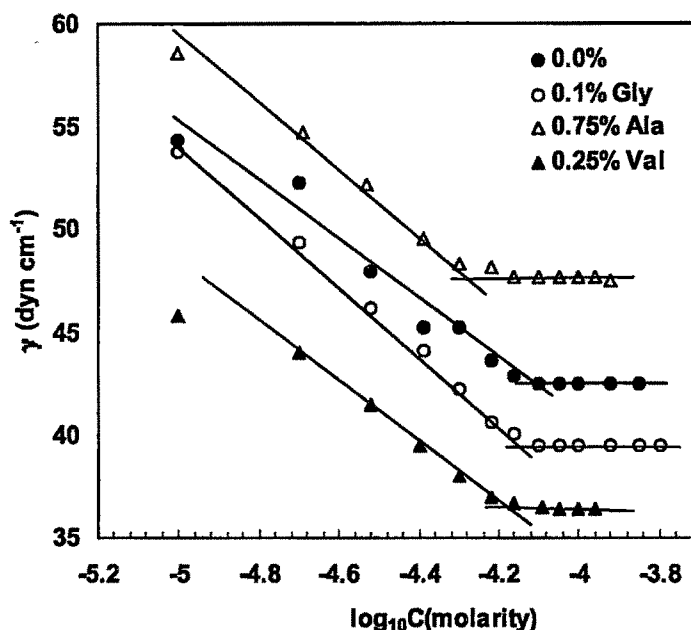


Figure 3. Representative plot of surface tension vs  $\log_{10}C$  in presence of different amino acids at 35°C.

The cmc value of  $C_{12}E_9$  was found to be 0.079mM at 35°C, which is good agreement with the earlier reported value.<sup>41</sup> The literature value of cmc of  $C_{12}E_9$  is 0.1mM at 23°C reported by Lange et al<sup>42</sup>. However, we determined the cmc at 35°C, so it is obvious as in the case of nonionic surfactant that the cmc value decreases on increase in temperature. In the case of aquo-amino acids systems, the cmc values decrease progressively by increasing the concentration of amino acids. In the presence of amino acids the cmc values depend up on the surfactant as well as to the structural modification of the solvent surrounding the micelle. It is well known that amino acids are efficient water structure breaking agents. Thus it is expected to decrease the solubility of the hydrocarbon tails of the surfactant, as well as to increase interfacial tension between the micellar hydrophobic core and aqueous solvent. Both these effect could be responsible for the decrease of the cmc of  $C_{12}E_9$ .

The cmc of  $C_{12}E_9$  decreases by 25% on adding 1% of gly, while 1% val decrease it by 29%. Bakshi et al <sup>25</sup> registered the decrease in cmc of SDS and DTAB by 0.17M gly by 7.4% and 10.4% respectively, by conductance measurements. The authors concluded that the cmcs of both SDS and DTAB decreased upon the addition of ala, val and methionine. However they found that the effect of these additives were much stronger in the case of DTAB rather than in the case of SDS. However in the present case the cmcs are reduced by 25-29%. Such predominant effect of amino acids can be attributed to their strong structure breaking<sup>20</sup> effects, which is significant in aqueous  $C_{12}E_9$  nonionic surfactant than ionic one. However, the effect of gly on the micellization remain relatively less stronger in comparison to other amino acids which could be due to contribution of solvophobic interactions since gly is the first member of the neutral amino acids category<sup>20</sup> having no alkyl group attached to it. It has been pointed out by us <sup>7,8,11</sup> that the addition of the additive breaks the water matrix. Moreover, there will be a formation of structure between the free water molecules and the additive, particularly those having hydrogen-bond-forming groups, as in the present case. Moreover, cosolubilization as well as mixed micelle formation are also possible. In other words the micellization in these systems is complicated one.

Table 1 also lists the value of  $CMC/C_{20}$ , which is a measure of the tendency of the surfactant to adsorb at the air/solution interface relative to its tendency to form micelles. It can be seen from Table 1 that the  $CMC/C_{20}$  of the pure  $C_{12}E_9$  is 3.43, and in the presence of amino acids this value in generally decrease in the case of gly and ala while for val it increases. An increase in  $CMC/C_{20}$  ratio in the presence of val indicates that the micellization is inhibited more than adsorption or adsorption is facilitated more than micellization.

Table 1

Various Physicochemical parameters for C<sub>12</sub>E<sub>9</sub> Amino acids System at 35°C.

gly(%)	CMC (10 <sup>-3</sup> M)	C <sub>20</sub> (10 <sup>-5</sup> M)	CMC/C <sub>20</sub>	π <sub>cmc</sub> (dyne cm <sup>-1</sup> )	Γ <sub>max</sub> ×10 <sup>10</sup> (molem <sup>-2</sup> )	A <sub>min</sub> (nm <sup>2</sup> )	ΔG <sub>m</sub> <sup>o</sup> (kJmol <sup>-1</sup> )	ΔG <sub>ad</sub> <sup>o</sup> (kJmol <sup>-1</sup> )	ΔG <sub>m</sub> <sup>o</sup> -ΔG <sub>ad</sub> <sup>o</sup> (kJmol <sup>-1</sup> )	σ <sub>ox</sub> 10 <sup>-7</sup>
0.0	7.9±0.08	2.3	3.4	29.4	2.67	0.62	-34.5	-45.5	11.0	5.2
0.1	7.1±0.07	1.9	3.8	30.8	3.16	0.53	-34.7	-44.5	9.8	3.5
0.25	6.6±0.07	2.2	3.0	28.1	2.78	0.59	-34.9	-45.0	10.1	4.3
0.5	6.3±0.06	4.1	1.6	23.0	3.01	0.55	-35.1	-42.7	7.6	1.7
0.75	5.9±0.06	5.7	1.0	20.3	2.90	0.57	-35.3	-42.3	7.0	1.5
1.0	5.9±0.06	5.1	1.2	21.6	2.73	0.61	-35.3	-43.2	7.9	2.1
ala										
0.1	6.5±0.07	5.1	1.3	21.8	4.59	0.36	-35.0	-39.7	4.7	0.5
0.25	6.3±0.06	4.7	1.4	22.7	3.89	0.43	-35.1	-40.9	5.8	0.9
0.5	5.9±0.06	5.8	1.0	20.3	4.28	0.39	-35.3	-40.1	4.8	0.6
0.75	5.7±0.06	3.7	1.5	22.6	3.19	0.52	-35.3	-42.4	7.1	1.6
1.0	6.0±0.06	5.7	1.1	21.4	4.01	0.41	-35.2	-40.5	5.3	0.7
val										
0.1	6.9±0.07	1.5	4.7	32.1	3.82	0.44	-34.9	-43.3	8.4	2.2
0.25	6.6±0.07	0.7	9.7	33.7	4.27	0.39	-34.9	-42.8	7.9	1.8
0.5	5.9±0.06	1.2	5.1	32.1	3.24	0.51	-35.3	-45.2	9.9	4.7
0.75	5.9±0.06	1.6	3.6	27.8	2.93	0.57	-35.3	-44.8	9.5	3.9
1.0	5.6±0.06	1.6	3.6	29.5	3.28	0.51	-35.4	-44.3	8.9	3.3

\* ref 41

The surface excess concentration,  $\Gamma_{\max}$ , of the surfactant molecules in the surface layer compared to the bulk, the area per molecule,  $A_{\min}$  in the surface monolayer were calculated by the standard procedure<sup>6</sup>. The slope of the tangent at the given concentration of the  $\gamma$  vs.  $\log C$  plot has been used to calculate  $\Gamma$ , by using curve fitting to a polynomial equation of the form,  $y = ax^2 + bx + c$  in microsoft excel program. The  $R^2$  (Regression coefficient) value of the fit lies between 0.9743 and 0.9997. The  $\Gamma_{\max}$  and  $A_{\min}$  values are presented in columns 6 and 7 of Table 1. In general it is observed that the  $\Gamma_{\max}$  quantity increased relatively and correspondingly  $A_{\min}$  decreases with addition of amino acids. This may result by removal of water from the ethoxy segment of the nonionic surfactant, hence the tendency to locate at the air/water interface become higher. The magnitude of  $A_{\min}$  is much less than  $1.0 \text{ nm}^2$ , suggesting that the air/water interface is a close packed one and therefore the orientation of the surfactant molecule is almost perpendicular to the surface.

The effectiveness of a surface-active molecule is measured by surface pressure at the cmc,  $\pi_{\text{cmc}} (= \gamma_0 - \gamma_{\text{cmc}})$ , where  $\gamma_0$  and  $\gamma_{\text{cmc}}$  are the surface tension of water and surface tension at cmc respectively. The value  $\pi_{\text{cmc}}$  were found to be maximum in the case of val (Table 1) which show that  $\text{C}_{12}\text{E}_9$  is much effective in val while less in the case of gly and ala.

The free energy of micellization,  $\Delta G_m^0$ , and adsorption at air/water interface,  $\Delta G_{ad}^0$  were calculated by standard relations.<sup>6</sup> Column 8-10 of the Table 1 shows the values of  $\Delta G_m^0$ ,  $\Delta G_{ad}^0$  and the difference in both. It can be observed that the  $\Delta G_m^0$  values are found more negative in the presence of an additive that is the formation of micelles becomes relatively more spontaneous and stable in the presence or absence of amino acids. This can be attributed to the energy associated with the transfer of hydrophobic tails from the medium to the micelle that seem to be more



favourable in the case of val. It is also found that the values of  $\Delta G_{ad}^o$  were negative throughout, indicating that the adsorption of the surfactant at the air/water interface took place spontaneously in the presence of amino acids. As expected  $\Delta G_{ad}^o$  values were found to be more negative than the corresponding  $\Delta G_m^o$  values. This indicates that the surfactant molecules prefer to reside at the surface and work has to be done for transferring the individual surfactant molecules to the micelles. Under this condition the interface was saturated with monomeric surfactant molecules. In absence of any additive the difference between  $\Delta G_m^o$  and  $\Delta G_{ad}^o$  is higher than in presence of amino acids.

It has been further suggested by Weiner et al <sup>43</sup> that,

$$\Delta G_{ad}^o = -RT \ln \sigma \quad (1)$$

where ' $\sigma$ ' is known as Traube's constant<sup>4</sup> and is defined by the relation

$$\sigma = (\partial \pi / \partial C)_{C \rightarrow 0} = -(\partial \gamma / \partial C)_{C \rightarrow 0} \quad (2)$$

This means that  $\sigma$  is the rate of change of surface pressure per unit concentration change at infinite dilution. It can be noted that the value of  $\sigma$  (column 11 of Table 1) of the pure  $C_{12}E_9$  is similar to the data given in Table 4 of Meguro et.al<sup>44</sup> there by suggesting that our adsorption data are reasonable. We computed the effect of different amino acids on  $\sigma$ . It seems that there is difference in  $\sigma$  values as a function of amino acids, probably because the additives are taking role in the adsorption processes. However the value of  $\sigma$  is found to lower in the presence of amino acids.

### Small Angle Neutron Scattering (SANS) Study of C<sub>12</sub>E<sub>9</sub>: Effect of Amino acids and Temperature on the C<sub>12</sub>E<sub>9</sub> micelles.

**SANS Data Analysis.** In SANS experiments, the coherent differential scattering cross-section per unit volume ( $d\Sigma/d\Omega$ ) for a solution of monodisperse micelles is given by <sup>45,46</sup>.

$$d\Sigma/d\Omega = n_m (\rho_m - \rho_s)^2 V^2 \left[ \langle F^2(Q) \rangle + \langle F(Q) \rangle^2 (S(Q) - 1) \right] + B \quad (3)$$

where  $n_m$  denotes the number density of the micelles,  $\rho_m$  and  $\rho_s$  are the scattering length densities of the micelles and the solvent, respectively and  $V$  is the volume of the micelle.  $F(Q)$  is the single particle (intraparticle) form factor, and  $S(Q)$  is the interparticle structure factor.  $B$  is a constant term that represents the incoherent scattering back ground, which is mainly due to the hydrogen in the sample. The particle form factor  $F(Q)$  depends on the shape and size of the micelles. Expression for  $F(Q)$  corresponding to different geometrical shape are known.<sup>47</sup> In particular,  $F(Q)$  for an ellipsoidal micelle is given as<sup>33C</sup>

$$\langle F^2(Q) \rangle = \int_0^1 [F(Q, \mu)]^2 d\mu \quad (5)$$

$$\langle F(Q) \rangle^2 = \left[ \int_0^1 F(Q, \mu) d\mu \right]^2 \quad (6)$$

$$F(Q, \mu) = \frac{3(\sin x - x \cos x)}{x^3} \quad (7)$$

$$x = Q[a^2 \mu^2 + b^2 (1 - \mu^2)]^{1/2} \quad (8)$$

where  $a$  and  $b$  are, respectively, the semimajor and semiminor axis of the ellipsoidal micelle and  $\mu$  is the cosine of the angle between the major axis and the wave vector transfer  $Q$ .  $S(Q)$ , the interparticle structure factor, is decided by the spatial arrangement of micelles in solution. Usually  $S(Q)$  shows a peak at  $Q_m = 2\pi/D$ , where  $D$  is the average distance between the micelles in the case of the ionic surfactant. It can be mentioned that the spatial arrangement of micelles

and the  $S(Q)$  depends on the intermicellar interaction. In general, the interaction potential,  $V(r)$ , between micelles could change with temperature of the solution. That is a change in temperature could also result in change in  $S(Q)$ .

The SANS distribution plots of  $d\Sigma/d\Omega$  vs  $Q$  for aqueous  $C_{12}E_9$  surfactant solution at different concentrations (5, 10 and 20mM) at 30°C, 20mM at different temperatures (30, 45 and 60°C), in presence of val (0.4M) at different temperatures (30, 45 and 60°C) and in presence of different amino acids at 30°C are shown in Figures 4-6, respectively. There is no indication of any correlation peak, which suggest that for the concentrations of surfactant and amino acids reported in this work, intermicellar interference effect are negligible. Thus we have assumed  $S(Q)=1$  in further analysis. The eqn 3 gets reduced to

$$d\Sigma/d\Omega = n_m V_m^2 (\rho_m - \rho_s)^2 \langle F^2(Q) \rangle + B \quad (9)$$

The micelles formed by the  $C_{12}E_9$  surfactant consist of a core made of hydrophobic dodecyl group and hydrophilic nona oxyethylene. The scattering length density of hydrophobic part ( $\rho_m$ ) is calculated to be  $1.89 \times 10^{10} \text{ cm}^{-2}$ . The scattering length density of  $D_2O$  ( $\rho_s$ ) is  $6.38 \times 10^{10} \text{ cm}^{-2}$ . Thus, there is very good contrast between the hydrophobic part of the micelle and  $D_2O$ . Since, the outer shell of the micellar associates is expected to be swollen extensively with water ( $D_2O$ ), the scattering contrast between the outer shell of the associates and the solvent could be very poor. In view of this and as considered in the literature<sup>48</sup> we assume that the  $F(Q)$  value depends mainly on the micellar core dimensions. The correlation between calculated and experimental values of scattering intensities is judged by calculating  $\chi^2$  values using the nonlinear least square fitting.

$$\chi^2 = (1/M - K) \Sigma [I_{cal} - I_{exp} / (E(I_{exp}))]^2$$

It was found that our experimental SANS intensity were best matched with the values obtained by using prolate ellipsoidal model. The aggregation number ( $N_{agg}$ )

for the micelle is related to the micellar volume ( $V_m$ ) by the relation,  $N_{agg}=V_m/ v^{11}$ , where  $V_m = 4/3\pi a b^2$  and  $v$  is the volume of the single surfactant monomer at a given temperature. The value of  $v$  calculated by Tanford formula<sup>49</sup> ( $v=27.4+26.9n$ , where  $n$ =number of carbon atom in hydrophobic part, in the present case it is 12) is  $350.2 \text{ \AA}^3$  and  $a$  and  $b=c$  are the *semimajor* and *semiminor* axes, respectively. The scattering length of hydrophobic part of surfactant calculated by Tanford formula<sup>49</sup> ( $=1.5+1.265n$ , where  $n$  is number of carbon atom in hydrophobic part, which is 12) is  $16.7 \text{ \AA}$ , considered as semi minor axis ( $b=c$ ) as constant (see Table 2).

**Table 2**

SANS parameters of C<sub>12</sub>E<sub>9</sub> Micellar System at Different Temperature and in the Presence of Amino acids.

Micellar system C <sub>12</sub> E <sub>9</sub> (20mM) (°C)	a (Å)	b=c (Å)	N <sub>agg</sub>	a/b	N <sub>m</sub> (X10 <sup>16</sup> cm <sup>-3</sup> )
30	46.1 ±2.3	16.7	154 ±8	2.76 ±0.14	7.8 ±0.39
45	48.9 ±2.4	16.7	163 ±8	2.93 ±0.19	7.4 ±0.37
60	78.4 ±3.9	16.7	261 ±13	4.69 ±0.23	4.6 ±0.23
C <sub>12</sub> E <sub>9</sub> (mM) at 30°C					
5	47.2 ±2.4	16.7	157 ±8	2.83 ±0.14	1.9 ±0.09
10	46.8 ±2.3	16.7	156 ±8	2.80 ±0.14	3.9 ±0.19
20	46.1 ±2.3	16.7	154 ±8	2.76 ±0.14	7.8 ±0.39
C <sub>12</sub> E <sub>9</sub> (20mM)+ Amino acids at 30°C					
gly (0.4M)	48.5 ±2.4	16.7	161 ±8	2.90 ±0.15	7.4 ±0.37
ala (0.4M)	50.4 ±2.5	16.7	168 ±8	3.02 ±0.15	7.2 ±0.36
val (0.4M)	47.1 ±2.4	16.7	157 ±7	2.82 ±0.14	8.0 ±0.40
gly (0.6M)	50.9 ±2.5	16.7	170 ±8	3.05 ±0.15	7.1 ±0.36
ala (0.6M)	53.0 ±2.7	16.7	177 ±9	3.17 ±0.16	6.8 ±0.34
C <sub>12</sub> E <sub>9</sub> (20mM)+val (0.4M) (°C)					
30	47.1 ±2.4	16.7	157 ±8	2.82 ±0.14	8.0 ±0.40
45	51.8 ±2.6	16.7	172 ±9	3.01 ±0.15	7.0 ±0.35
60	85.5 ±4.3	16.7	285 ±14	5.12 ±0.26	4.2 ±0.21

From the calculated values of  $N_{agg}$ , the number density of micelles,  $n_m$  is calculated by the following relation<sup>11</sup>

$$n_m / \text{cm}^{-3} = \frac{(C - \text{CMC}) \times 10^3 N_A}{N_{agg}} \quad (11)$$

where  $C$  = concentration of surfactant in mole lit<sup>-1</sup> and  $N_A$  = Avogadrs number. Under the condition  $S(Q) = 1$ , a look at eqn 9 used for evaluating the theoretical scattering reveals that the  $d\Sigma/d\Omega$  can be considered proportional to  $F(Q)$  when the terms  $n_m$ ,  $V_m$ , and  $(\rho_m - \rho_s)$  are constants. As the shape and size of micelles and hence  $F(Q)$  do not change with concentration, the observed enhance intensities can be accounted by a corresponding change in the number density of micelles. Indeed the last column of Table 2 shows about a 4-fold increase in  $n_m$  values when the

concentration is varied from 5 to 20mM. The theory of micellization based on the closed association model predicts a similar increase in the number density of nonspherical globular (or ellipsoidal) micelle with increase in concentration.<sup>50</sup>

**Temperature and Amino Acids Dependence.** The scattering curves for a fixed concentration 20mM (~1.17%) of C<sub>12</sub>E<sub>9</sub> aqueous solution was also obtained at 45 and 60°C. The curve at 30, 45 and 60°C are shown in Figure 4. It is seen that SANS intensity at large Q values are independent of temperature. However, at low Q, the SANS intensity increase as one approaches the cloud point. In the principle, this cloud happen either because of a change in  $F(Q)$  (i.e. because of change in micellar growth) or because of a change in  $S(Q)$  (i.e. because of change in the intermicellar interaction potential). SANS data have been analyzed in the literature using both approaches, namely, one based on micellar growth or one based on divergence of  $S(Q)$ . It seems SANS data can not distinguish the two models though one can get certain parameters. We have interpreted the SANS data in terms of micellar growth for the following reasons: (i) the measured SANS distributions do not show a correlation peak indicating that the intermicellar structure factor  $S(Q)$  is not important, and (ii) the viscosity data show that there is a growth of the micelle as one approaches cloud temperature (see the next section).

The micellar parameters at different temperatures are given in Table 2. Table 2 shows that on increasing the temperature from 30 to 60°C, the semimajor axis and the  $N_{agg}$  are increased by 70%. This indicates that a lateral elongation of the micelle take palce by the taking more and more surfactant molecules and hence the  $n_m$  decreases. However at the same concentration (0.4M) from gly to val the axial ratio is in the range from 2.9 to 3.02 which show that val is bigger molecule and it occupies the more space in micelle. The micelles were found to be ellipsoid at 30°C, however they become rod-like with  $a/b \sim 5$  both in presence and absence

of amino acids on increasing the temperature from 30 to 60°C. The polyoxyethylene (POE) moiety of nonionic surfactant is less hydrated at a higher temperature, therefore on heating a dilute solution of polyoxyethylated surfactant the tendency towards self-association increase, thereby decreasing the cmc and increasing the size of the micelle<sup>7</sup>. Thus again, we analyzed the measured distributions of C<sub>12</sub>E<sub>9</sub> aqueous solution in the presence of amino acids at a fixed temperature as well as at different temperatures keeping the concentration of val constant using eqn 9 assuming ellipsoidal micelles. Because of the fact that large Q data are independent of temperature (Figure 5), the value of semiminor axis was fixed to  $b = 16.7 \text{ \AA}$ .

It can also be seen that the semimajor axis  $a$  registered an increase of 82% with val and 70% without amino acids, rise in temperature from 30 to 60°C. Accordingly, the axial ratio  $a/b$  increase substantially. It is well known that at elevated temperatures dehydration not only cause conformational changes but also even disturb the geometry.<sup>51</sup> Extensive SANS measurements<sup>48b, 52</sup> on pluronic family of surfactants have been made. It has been reported that in most cases the micelles formed were of hard spherical type in shape and that a rise in temperature (i) systematically increased various micellar parameters and (ii) causes spherical micelles in some cases to even undergo a sphere to rod transition. Similarly, several authors,<sup>53-55</sup> analyzed the SANS intensities from spherical micelles, allow for water in the core. Thus, both core as well as corona parts undergo dehydration at elevated temperature. We could not ascertain the information on the exact nature of the core and corona because of the poor contrast between the corona and the solvent medium. Table 2 reveals that the elongation along the semimajor axis of the aggregates systematically increases the aggregation number,  $N_{agg}$ , and decreases the number density of the micelles at elevated temperatures. The increased  $N_{agg}$  values indicate that more surfactant molecules have been added into the space created because of the expulsion of water probably from the core as well

as parts of the corona portions of the micelles. The increase size of the aggregates as observed should decrease the number of aggregates in unit volume, i.e. number density,  $n_m$  which was also observed. The broad spacing of the aggregates (low number density values) interspersed by water molecules (from bulk media) means absence of spatial correlation among the nearest neighbors, as evidenced by the absence of the correlation peak in curves shown in Figures 4-6.

The observed elongation of the semimajor axis could be attributed to the loss of water (if any) from the core part, causing an expansion of hydrophobic chains or the merger of the part of dehydrated OE chains into the core part alongside the interface between the hydrophobic and hydrophilic regions. The dehydration effect more in the presence of amino acids, result the bigger sized particles as evidence by higher  $a$  values of 78.4 Å in pure C<sub>12</sub>E<sub>9</sub> in comparison to a value of 85.5 Å in presence of val at 60°C.



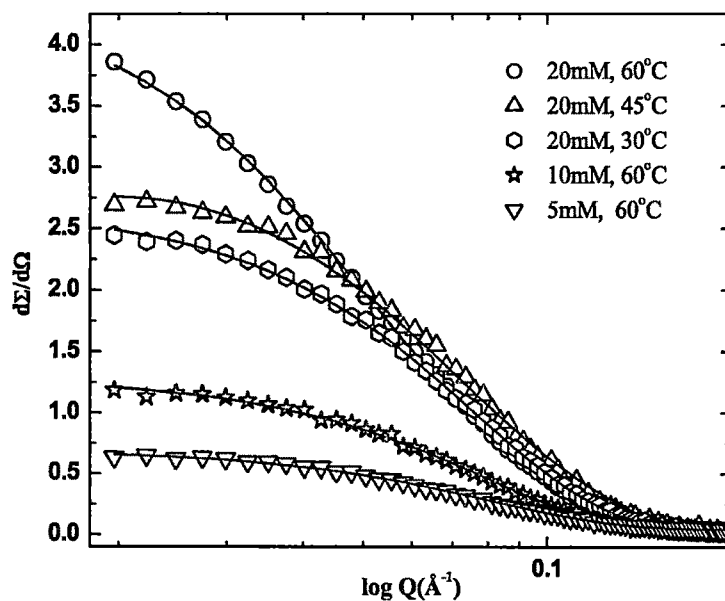


Figure 4. SANS distribution for  $C_{12}E_9$  at different temperatures and concentrations.

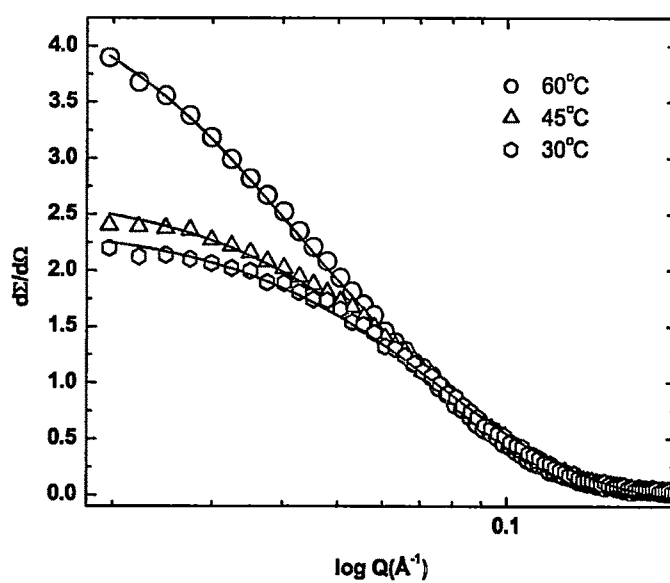


Figure 5. SANS distribution for  $C_{12}E_9$  (20mM) in presence of Val (0.4M) at different temperatures. The solid lines are theoretical fit and the symbols are experimental values.

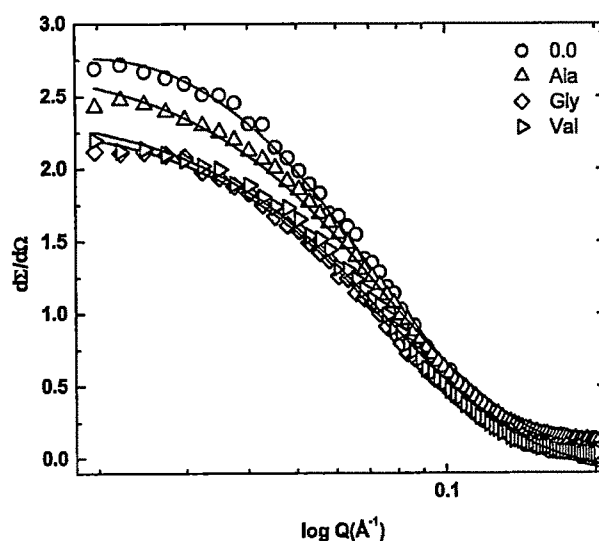


Figure 6. SANS distribution for  $C_{12}E_9$  (20mM) in presence of amino acids (0.4M) at  $30^\circ\text{C}$ . The solid lines correspond to the fits to the model as described in text and the symbols are experimental values.

Model fitting of SANS data showed that the surfactant formed prolate ellipsoidal micelle with a constant size (in the concentration range of 5mM to 20mM) but the micelle registered a 60 - 70% increase in size, in the association number and the other micellar parameter (i.e. the number density of micelles changed inversely with the rise in temperature) from  $30$  to  $60^\circ\text{C}$ , rise in temperature. The changes in the parameters have been interpreted mainly in terms of dehydration effects at elevated temperature as also observed from the viscosity data.

**Viscosity.** Viscosity measurements provide very useful information on the hydrodynamic volume of micellar aggregates. The viscosities of aqueous solution (5, 10 and 20mM) of  $C_{12}E_9$  surfactant, at the three temperatures, and in the presence of amino acids have been measured at which SANS and DLS measurements were made. The intrinsic viscosity  $[\eta]$  calculated using the

relation,

$$|\eta| = \lim_{C \rightarrow 0} (\eta_r - 1)/C \quad (12)$$

where limit to zero concentration indicates that intermolecular interactions are absent and  $\eta_r$  indicates the relative viscosity of the surfactant solution respectively. Some researchers<sup>56,57</sup> have taken  $|\eta|$  to be equal to  $(\eta_r - 1)/C$  without the condition of limiting concentration. In this article we have calculated  $|\eta|$  without taking the zero concentration limit as we did earlier.<sup>11</sup>

The intrinsic viscosity  $|\eta|$  decrease with an increase in temperature, indicating pronounced micellar dehydration (Table 3). It is well known that the viscosity of a liquid decreases with rise in temperature. Also on increasing temperature the random movement of solute surfactant molecules take place because of increasing kinetic energy. The micelles become compact with an increase in temperature due to dehydration of OE chains. In presence of amino acids similar behavior with respect to temperature has been observed. However  $|\eta|$  value increase due to the cosolubilization on increasing the concentration of amino acids.

**Table 3**  
Rheological and Dynamic Light Scattering Parameters of C<sub>12</sub>E<sub>9</sub> Micellar System at different Temperatures and in the Presence of Amino acids.

C <sub>12</sub> E <sub>9</sub> (20mM) °C	$ \eta $ cm <sup>3</sup> /g	$V_h$ x10 <sup>4</sup> Å <sup>3</sup>	$V_c$ x10 <sup>4</sup> Å <sup>3</sup>	$V_{OE}$ x10 <sup>4</sup> Å <sup>3</sup>	$V_{OE}/V_h$	D 10 <sup>-4</sup> cm <sup>2</sup> s <sup>-1</sup>	$R_h$ nm
30	6.88	40.9	5.87	35.0	0.86	69.9	3.5
45	3.79	23.9	6.22	17.7	0.74	89.9	2.7
60	1.53	15.5	9.99	5.5	0.35	110.0*	2.2*
C <sub>12</sub> E <sub>9</sub> (mM) at 30°C							
5	4.72	28.6	5.99	22.6	0.79	85.6	2.9
10	5.11	30.8	5.95	24.9	0.81	79.8	3.1
20	6.88	40.9	5.87	35.0	0.86	69.9	3.5
C <sub>12</sub> E <sub>9</sub> (20mM)+ Amino acids at 30°C							
Gly (0.4M)	10.4	65.1	6.18	58.9	0.90	77.7	3.2
Ala (0.4M)	14.4	93.5	6.41	87.1	0.93	59.8	4.1
Val (0.4M)	8.06	47.0	5.76	41.2	0.88	70.3	3.9
Gly (0.6M)	13.4	88.0	6.48	81.5	0.92	78.4	3.6
Ala (0.6M)	16.3	11.5	6.75	104.8	0.94	62.9	4.3
C <sub>12</sub> E <sub>9</sub> (20mM)+Val (0.4M) (°C)							
30	8.06	47.0	5.76	41.2	0.88	70.3	3.5
45	6.32	42.0	6.56	35.4	0.84	86.6	2.8
60	3.68	40.5	10.87	29.6	0.73	90.7*	2.7*

\* Temperature at 55°C

Among the amino acids used, the variation is in the order of ala>gly>cys. From intrinsic viscosity the hydrated micellar volume ( $V_h$ ) have been computed by the relation<sup>8</sup>

$$V_h = |\eta| M_m / 2.5 N_A \tag{13}$$

where  $M_m$  ( $=N_{agg} M$ ) is the micellar molecular weight,  $N_{agg}$  is the aggregation number obtained by SANS studies (taken from Table 6) and  $M$  is the molecular weight of C<sub>12</sub>E<sub>9</sub>

The volume of the hydrocarbon core ( $V_c$ ) and the volume of the palisade layer of ethylene oxide units ( $V_{OE}$ ) have been calculated using the following equations<sup>8</sup>

$$V_c = A_n V = 10^{24} A_n M_c / d N \quad (14)$$

$$\text{and} \quad V_{OE} = V_h - V_c \quad (15)$$

where  $V$  is the volume of alkyl chain length in a single  $C_{12}E_n$  molecule,  $M_c$  is the molecular weight (170) and  $d$  is the density of the corresponding liquid  $n$ -alkane at different temperatures as mentioned earlier<sup>8</sup>. The  $V_h$  and  $V_{OE}$  units decrease as the temperature increases both in presence and absence of amino acids, while  $V_c$  increases. This occurred because the  $N_{agg}$  of the micelle increased, which attributed to increase in size. Obviously, with an increase in temperature,  $V_c$  should increase, and that is what we observe (Table 3). This may be because zwitterionic moiety of amino acids may interact with OE part of nonionic surfactant and find themselves at the micelle-water interface. On increasing temperature both  $V_h$  and  $V_{OE}$  increase. This is because the  $N_{agg}$  of the micelle increases, explained in an earlier paragraph. It is obvious that with increase in temperature  $V_c$  should increase and that is observed. The variation of  $V_{OE}/V_h$  ratio with temperature is a function of size and nature of the additive.

**Quasielastic Light Scattering (QELS).** The normalized time correlation function of the scattered intensity,  $g^{(2)}(\tau)$  can be written as<sup>58</sup>

$$g^{(2)}(\tau) = \frac{\langle I(0)I(\tau) \rangle}{\langle I \rangle^2} \quad (16)$$

For a suspension of monodisperse, rigid, spherical particles undergoing Brownian diffusion, the correlation function decays exponentially and is given as

$$g^{(2)}(\tau) = A \cdot \exp(-Dq^2\tau) + B \quad (17)$$

where  $A$  is amplitude,  $B$  is base line,  $D$  is the translation diffusion coefficient and  $q$  is the magnitude of the scattering wave vector and in DLS given by  $q = (4\pi n/\lambda) \sin(\theta/2)$ . Where  $n$  = refractive index of the solvent (1.33 for water at 30°C).

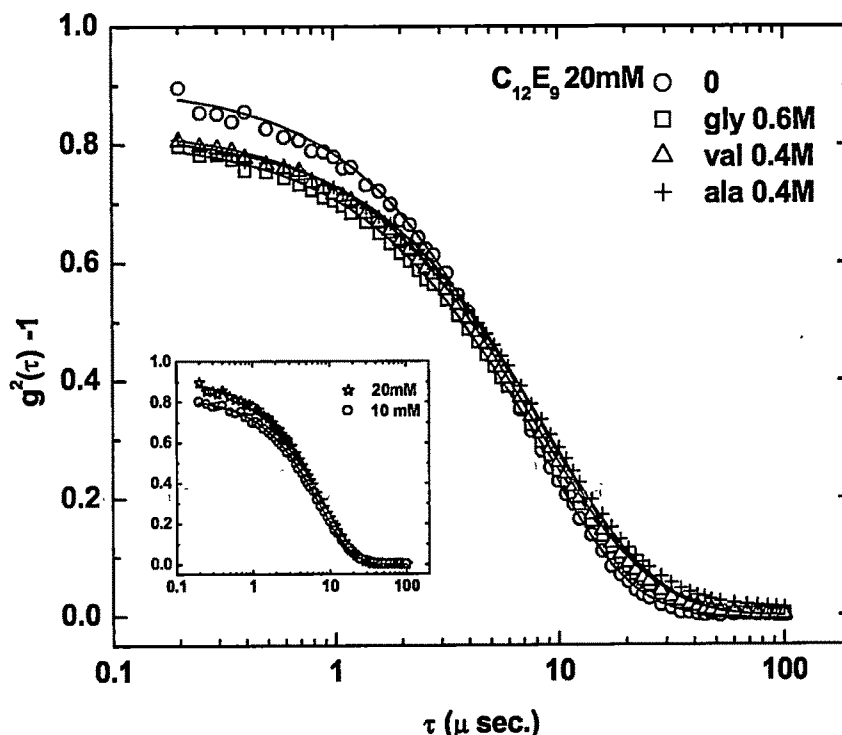


Figure 7. Correlation function vs time (semi logarithmic) for the scattered light intensity from  $C_{12}E_9$  aqueous surfactant solution in presence of amino acids system at 25°C and 130° angle. The solids lines are fit to the experimental data with a single-exponential decay.

Figure 7 shows the representative curves of the normalized time correlation of the light intensity scattered at angle of 130° at 30°C from 20mM standard  $C_{12}E_9$  solution in the presence of gly (0.6M), ala (0.4M) and val (0.4M) solutions. As seen from the inset of Figure 7, the time profiles are also well represented by a single relaxation time for pure  $C_{12}E_9$  (10 and 20mM) system. Similar results were observed at 5mM surfactant concentration and at different temperatures. The solid lines in the figure correspond to the decay patterns of the correlation function calculated from assuming a unimodel distribution decay. These lines are drawn from a best least square fit analysis to the data with a single diffusion coefficient

( $D_0$ ). Figure 8 represents the average decay rates of intensity correlation functions ( $\Gamma$ ) as a function of  $q^2$  for 20mM  $C_{12}E_9$  surfactant system. The diffusion coefficient ( $D_0$ ) values were obtained from the slope of  $\Gamma$  vs  $q^2$  plot. The diffusion coefficient ( $D_0$ ) for  $C_{12}E_9$  surfactant system, were evaluated by plotting diffusion coefficient extrapolating to zero concentration.

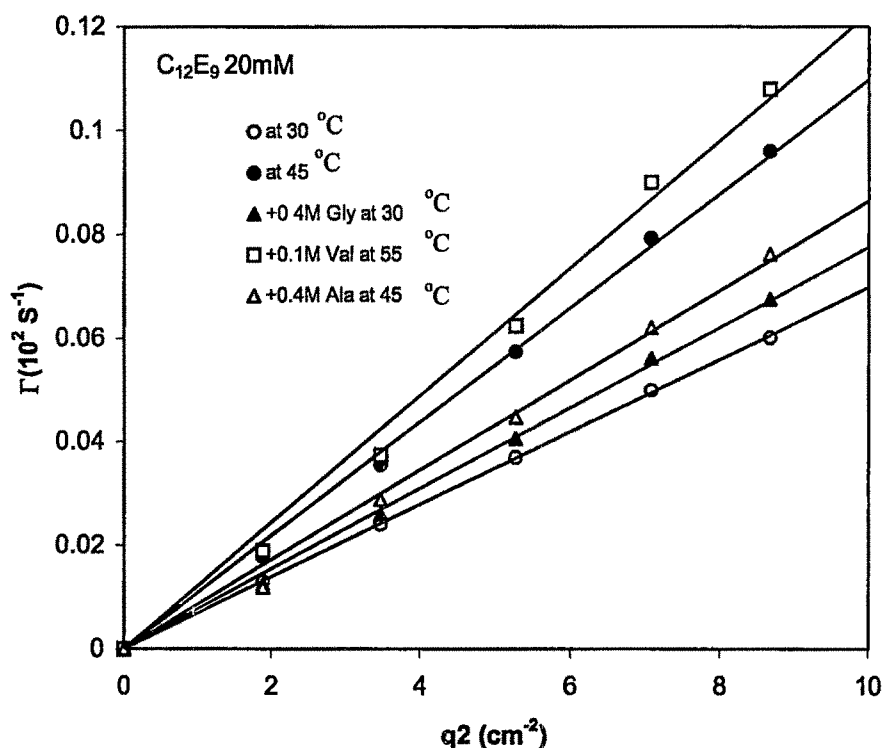


Figure 8. Average decay rate of the intensity correlation function ( $\Gamma$ ) as a function of  $q^2$  for 20mM  $C_{12}E_9$  with varying amino acids.

Translational diffusion coefficient values thus obtained were used to calculate the hydrodynamic radius of the micelle by applying well known Stokes-Einstein equation

$$R_h = \frac{kT}{6\pi\eta_o D_0} \quad (18)$$

where  $k$  is the Boltzman constant,  $\eta_o$  is the solvent viscosity and  $T$  is the absolute

temperature. The calculated data for diffusion coefficient ( $D_o$ ) and hydrodynamic radius ( $R_h$ ) from DLS at different angles are presented in column 7 and 8 of Table 3.

It is found that on increasing the concentration there is decrease in the diffusion coefficient (Table 3). Such a decrease of the diffusion coefficient with an increase of the surfactant concentration indicates that the diffusion of the particles deviates from the normal diffusion and the micro structure of the assemblies in the solution becomes changed.

We have also studied the effect of temperature on the hydrodynamic radius and diffusion of  $C_{12}E_9$  micelles in the absence and presence of amino acids as we did in SANS and viscosity studies. It is observed that in the case of  $C_{12}E_9$  self organized assemblies, the micellar length is a function of temperature. This dependence of the micellar length with temperature arises from the fact that the micelles are dynamic species that undergo braking and recombination within a characteristic time scale.<sup>54</sup> An increase of temperature favors the breaking of the micelles, and subsequent decrease of the average micellar length is observed. This is reflecting an increase in the average diffusion coefficient of the micelles. Similar effect was seen in the presence of val (0.4M), i.e the diffusion coefficient increase on increasing the temperature, while  $R_h$  decrease.



## CONCLUSIONS

In the present investigation, an attempt has been made through surface tension, SANS, DLS and viscosity measurements to characterized the physicochemical properties of micellar solution and structural information of  $C_{12}E_9$  surfactant in absence and in the presence of different amino acids in the region of the phase diagram corresponding to transparent and isotropic states. The cloud point of the solution is a function of surfactant concentration and shows a minimum around 8% surfactant concentration. Amino acids effect the CP and among the amino acids used the order of the decreasing of CP of  $C_{12}E_9$  is gly>ala>val. It is clear that the val, among the amino acids used, is a more effective surface tension reducing agent than the others. The structure breaking ability of amino acids and its interaction with the oxyethylene group of the given surfactant are dominating factors in the micellization process. Free energy of micellization ( $\Delta G_m^0$ ) values are found more negative in the presence of additives, that is the formation of micelles becomes relatively more spontaneous and stable in the presence of amino acids. Model fitting of SANS data showed that the surfactant formed prolate ellipsoidal micelle with a constant size (in the concentration range of 5mM to 20mM) but the micelle registered a 60 - 70% increase in size, in the association number and the other micellar parameters with the rise in temperature from 30 to 60°C. It is observed the increase in the major axis of 82% with val and 70% without amino acids, (rise in temperature from 30 to 60°C) reveals that the elongation along the major axis of the aggregates systematically increases the aggregation number,  $N_{agg}$ , and decreases the number density of the micelles at elevated temperatures.

Rheological measurement shows that the  $V_h$ , and  $V_{OE}$  decrease as the temperature increases both in presence and absence of amino acids, while  $V_c$  increases. This happen because the  $N_{agg}$  of the micelle increased, which

attributed to increase in size, observed by SANS study. The value of hydrodynamic radius of micelle ( $R_h$ ) decrease on increasing the concentration of surfactant and also on increasing the temperatures.

## REFERENCES

- (1) Haldar, J.; Aswal, V. K.; Goyal, P. S.; Bhattacharya, S. *J. Phys. Chem. B* **2001**, *105*, 12803.
- (2) Degiorgio, V.; Corti, M. *Physics of Amphiphilies, Micelles, Vesicles and Micro emulsion*, North-Holland, Amsterdam, 1985.
- (3) Atwood, D.; Florence, A. T. *Surfactant Systems: Their Chemistry, Pharmacy and Biology*, Chapman and Hall, London, 1983.
- (4) Schick, M. J. *Micelle Formation in Aqueous Medium*, in *Nonionic surfactant, Physical Chemistry, Surfactant Science Series*, vol 23, Marcel Dekker, New York, 1987.
- (5). Moulik, S. P. Micelles: Self-Organized Surfactant Assemblies, *Current Science*, **1996** *71*, 368.
- (6). Rosen, M. J. *Surfactant and Interfacial Phenomena*, 2nd ed.; John-Wiley, New York, 1989.
- (7). Sulthana, S. B., Rao, P.V.C.; Bhat, S. G. T.; Rakshit, A. K. *J. Phys. Chem. B*, **1998**, *102*, 9653 and reference therein.
- (8). Sulthana, S.B., Bhatt, S.G.T.; Rakshit, A. K. *Langmuir* **1997**, *13*, 4562.
- (9). Sharma, K. S., Patil, S. R.; Rakshit, A. K. *Colloids Surf. A*, **2003**, *219*, 67.
- (10) Sharma, B. G.; Rakshit, A. K. *J. Colloid Interface Sci.* **1989**, *129*, 139.
- (11) Sharma, K. S.; Rakshit, A. K.; *J. Sur.t deterg.* **2004**, *7*, 305 and references there in.
- (12) Rakshit, A. K.; Sharma, B. *Colloid Poly. Sci.* **2003**, *281*, 45.
- (13) Mukerjee, P. *J. Phys. Chem.* **1965**, *69*, 4038.
- (14) Caponetti, E.; Causi, S.; deLisi, R.; Floriand, M.A.; Milioto, S.; Trido, R. *J. Phys. Chem.* **1992**, *96*, 4950.
- (15) Becher, P. In *Nonionic Surfactants* (ed. Schick, M.J.), M. Dekker, 1967, New York, ch.15.

- (16) Balles, B. L.; Ranganathan, R.; Griffiths, P.C. *J. Phys Chem. B*, **2001**, *105*, 7465.
- (17) Maltesh, C.; Somasundram, P. *Langmuir* **1996**, *8*, 1926.
- (18) (a) Meguro, K.; Ueno, M.; Esumi, K. in reference 6, p 151. (b) Ray, A. *Nature*, **1971**, *231*, 313. (c) Hamdiyyah, M. A.; Mansour, L. A. *J. Phys. Chem.*, **1979**, *83*, 2236.
- (19) Deguchi, K.; Mizuno, T.; Meguro, K. *J. Colloid Interface Sci.* **1974**, *48*, 474.
- (20) Lehninger, A. L.; Nelson, D. L.; Cox, M. M., *Principles of Biochemistry*, Worth publishers, USA, 1993.
- (21) Leodidis, E.B.; Hatton, T. A. *J. Phys. Chem.*, **1990**, *94*, 6400.
- (22) Leodidis, E.B.; Hatton, T. A. *J. Phys. Chem.*, **1990**, *94*, 6411.
- (23) Leodidis, E.B.; Bommarius, A. S.; Hatton, T. A. *J. Phys. Chem.*, **1991**, *95*, 5943.
- (24) Adachi, M.; Harada, M.; Shioi, A.; Sato, Y., *J. Phys. Chem.*, **1991**, *95*, 7925.
- (25) Bakshi, M.S.; Kohli, P. *Indian J. Chem A* **1997**, *36A*, 1075.
- (26) D'Aprano, A.; LaMesa, C.; Proletti, N.; Sesta, B.; Tatone, S. *J. Solution Chem.* **1994**, *23*, 1061.
- (27) (a) Evans, D.F.; Mitchell, D. J.; Ninham, B. W. *J. Phys. Chem.*, **1984**, *88*, 6344.
- (b) Lindman, B. Thalberg, K. In *Interaction of Surfactant with Polymers and Proteins*, Goddard, E.P. Anantha Padmanabhan, K. P. Eds, CRS Press, Boca Raton, FL 1993 p 203.
- (28) (a) Briganti, G.; Puvvada, S.; Blankschtein, D. *J. Phys. Chem.*, **1991**, *95*, 8989.
- (b) Briganti, G.; Bonincontro, A. *J. Non-Cryst. Solids* **1994**, *172*, 1173.
- (29) Vogel, I.; *Text book of Practical Organic Chemistry*, 5<sup>th</sup> Ed. Longman Sci & Technical, England. 1989.

- (30) Sharma, K. S.; Patil, S. R.; Rakshit, A. K.; Glenn, K.; Doiron, M.; Palepu, R. M.; Hassan, P. A. *J. Phys. Chem. B* **2004**, *34*, 12804.
- (31) Sharma, K. S.; Rodgers, C.; Palepu, R. M.; Rakshit, A. K. *J. Colloids Interface Sci.* **2003**, *262*, 482.
- (32) (a) Chen, S.H., *Annu. Rev. Phys. Chem.* **1986**, *37*, 351. (b) Hayter, J. B.; Penfold, J.J. *Colloid Polym. Sci.*, **1983**, *261*, 1072.
- (33) (a) Prasad, D.; Singh, H. N.; Goyal, P.S.; Rao, K.S. *J. Colloid Interface Sci.* **1993**, *155*, 415. (b) Kumar, S.; Aswal, V.K.; Goyal, P.S.; Kabir-ud-din, *J. Chem. Soc. Faraday Trans*, **1998**, *94*, 761. (c) Aswal, V. K. *J. Phys. Chem. B*, **2003**, *107*, 13323.
- (34) Aswal, V. K.; Goyal, P. S. *Current Science*, **2000**, *79*, 947.
- (35) Hassan, P. A.; Raghavan, S. R.; Kaler, E. W. *Langmuir* **2002**, *18*, 2543.
- (36) Koshy, L.; Saiyad, A. H.; Rakshit, A.K. *Colloid Polym. Sci*, **1996**, *274*, 582.
- (37) Heusch, R. *BTF-Biotech Forum* **1980**, *3*, 1.
- (38) Heusch R, *Naturwissenschaften* **1992**, *79*, 430.
- (39) Rupert, L. A. M. . *J. Colloid Interface Sci.* **1992**, *153*, 92.
- (40) Rakshit, A.K.; Palepu, R.M. in *Transworld Research Network, Recent Devel, Coll. Inter. Res.* **2003**, *1*, p 203.
- (41) Patil S R; Rakshit, A. K. *J. Indian Chem Soc.* **2003**, *80*, 345.
- (42) Lange H. *Kollid-Z* **1965**, *201*, 131.
- (43) Weiner, N. D.; Zografi, G. *J. Pharm. Sci.* **1965**, *54*, 436.
- (44) Ueno, M.; Takasawa, Y.; Miyashige, H.; Tabata, Y.; Meguro, K. *Colloid Polym. Sci.* **1981**, *259*, 761.
- (45) (a) Chen, S.H. *Annu. Rev. Phys. Chem.* **1986**, *37*, 351. (b) Chen, S. H.; Lin, T.L. *Methods of Experimental Physics*; Academic Press; New York, **1987**; Vol. 23B, p 489.
- (46) (a) Hayter, J.B.; Penfold, J. *J. Chem. Soc. Faraday Trans. I* **1881**, *77*, 1851.

- (b) Hayter, J. B.; Penfold, J. *J Mol. Phys.* **1981**, *42*, 109. (C) Hansen, J.P.; Hayter, J.B. *J. Mol. Phys.* **1982**, *46*, 109. (d) Hayter, J.B.; Penfold, J. *Colloid Polm. Sci.* **1983**, *261*, 1022.
- (47) Goyal, P.S. *Phase Transitions* **1994**, *50*, 143.
- (48) (a) Jain, N. J.; Aswal, V. K.; Goyal, P. S.; Bahadur, P. *J. Phys. Chem.* **1998**, *102*, 8452. (b) Mortensen, K.; Talmon, Y. *Macromolecules* **1995**, *28*, 8829.
- (49) Tanford, C. *The Hydrophobic Effect: Formation of Micelle and Biological Membranes*, Willey, New York, 1980.
- (50) Isralachivili, I.N.; Mitchell, D. J.; Ninham, B. W. *J. Chem Soc., Faraday Trans 2* **1976**, *72*, 1525.
- (51) Goyal, P.S.; Menon, S.V.G.; Dasannacharya, B.A.; Thiyagarajan, P. *Phys. Rev, E* **1995**, *51*, 2308.
- (52) Mortensen, K. *J. Phys. Condens. Matter* **1996**, *8A*, 103.
- (53) Goldmints, I.; von Gottberg, F.K.; Smith, K.A.; Hatton, T.A. *Langmuir* **1997**, *13*, 3659.
- (54) Goldmints, I.; Yu, G-E.; Booth, C.; Smith, K.A.; Hatton, T.A. *Langmuir* **1999**, *15*, 1651.
- (55) Pedersen, J.S.; Gerstenberg, M.C. *Macromolecules* **1996**, *29*, 1019.
- (56) Corti, M.; Minero, C.; V. Degiorgio, *J. Phys. Chem.* **1984**, *88*, 309.
- (57) Zulauf, M.; Rosenbusch, J. P. *J. Phys. Chem.* **1983**, *87*, 856.
- (58) Hassan, P.A.; Manohar, C. *J. Phys. Chem.* **1998**, *102*, 7120.